Defective peroxisomal catabolism of branched fatty acyl coenzyme A in mice lacking the sterol carrier protein-2/sterol carrier protein-x gene function

Udo Seedorf,[1,2,6] Martin Raabe,[1] Peter Ellinghaus,[1,7] Frank Kannenberg,[1] Manfred Fobker,[1,2] Thomas Engel,[1] Simone Denis,[3] Fred Wouters,[4] Karel W.A. Wirtz,[4] Ronald J.A. Wanders,[3] Nobuyo Maeda,[5] and Gerd Assmann[1,2]

[1]Institute for Arteriosclerosis Research and [2]Institute for Clinical Chemistry and Laboratory Medicine (Zentrallaboratorium), Westfalian Wilhelms-University, D-48129 Münster, Germany; [3]Department of Pediatrics, Academic Medical Center, University of Amsterdam, 1105 AZ Amsterdam, The Netherlands; [4]Center for Biomembranes and Lipid Enzymology, University of Utrecht, De Uithof, Utrecht, The Netherlands; [5]Department of Pathology, University of North Carolina at Chapel Hill, Chapel Hill, North Carolina 27599-7525 USA

Gene targeting in mice was used to investigate the unknown function of *Scp2*, encoding sterol carrier protein-2 (SCP2; a peroxisomal lipid carrier) and sterol carrier protein-x (SCPx; a fusion protein between SCP2 and a peroxisomal thiolase). Complete deficiency of SCP2 and SCPx was associated with marked alterations in gene expression, peroxisome proliferation, hypolipidemia, impaired body weight control, and neuropathy. Along with these abnormalities, catabolism of methyl-branched fatty acyl CoAs was impaired. The defect became evident from up to 10-fold accumulation of the tetramethyl-branched fatty acid phytanic acid in *Scp2*(−/−) mice. Further characterization supported that the gene disruption led to inefficient import of phytanoyl-CoA into peroxisomes and to defective thiolytic cleavage of 3-ketopristanoyl-CoA. These results corresponded to high-affinity binding of phytanoyl-CoA to the recombinant rat SCP2 protein, as well as high 3-ketopristanoyl-CoA thiolase activity of the recombinant rat SCPx protein.

[*Key Words:* Gene targeting; peroxisomes; β-oxidation; Refsum disease; cholesterol; steroid hormones]

Received December 10, 1997; revised version accepted February 9, 1998.

Sterol carrier protein-2 (SCP2) was isolated originally as a "cytosolic" factor required for efficient in vitro conversion of 7-dehydrocholesterol to cholesterol, catalyzed by microsomal sterol-Δ^7-reductase (Noland et al. 1980). Subsequently, it was shown that the protein was identical to the nonspecific lipid transfer protein (ns-LTP), which had been purified based on its ability to catalyze the exchange of a variety of phospholipids between membranes in vitro (Bloj and Zilversmit 1977). More recently, it could be demonstrated that purified SCP2 binds fatty acids and fatty acyl Coenzyme A (CoA) with similar or even higher affinity than sterols (Stolowich et al. 1997). Cloning and sequencing of SCP2 cDNAs showed that the protein comprises a carboxy-terminal SKL peroxisomal targeting signal (Seedorf and Assmann 1991), and immunocytochemical studies confirmed the predominant localization of SCP2 within peroxisomes (Keller et al. 1989; Ossendorp and Wirtz 1993). Several lines of indirect evidence exist that appear to support a role of SCP2 in adrenal and ovarian steroidogenesis (for review, see Pfeifer et al. 1993a). In addition, cell culture studies suggested a potential participation of SCP2 in cytosolic sterol transport to the plasma membrane (Puglielli et al. 1995; Baum et al. 1997). However, the localization of SCP2 in peroxisomes makes it difficult to understand how the protein might carry out these functions in the intact cell. Thus, the biological function of SCP2 is not clear.

The SCP2-encoding gene (*Scp2*) comprises 16 exons, spanning ~100 kb on human chromosome 1p32. Transcription initiation is controlled by two distant promoters that were mapped immediately upstream of the first exon (P1) and exon 12 (P2) (Ohba et al. 1994, 1995). P2 is used to generate SCP2-encoding transcripts, which com-

[6]Corresponding author.
E-MAIL seedorf@ear002.uni-muenster.de; FAX 49-251-8356208.
[7]This study contains part of a thesis work performed in partial fulfillment of the requirements of the Westfalian Wilhelms-University, Münster, Germany.

bine the coding information provided by exons 12–16. In addition, alternate transcription initiation at P1 leads to production of a second transcript that includes the coding information provided by exons 1–16. The respective gene product consists of 547 amino acids and was named sterol carrier protein-x (SCPx) (Seedorf and Assmann 1991). SCPx represents a fusion protein between a thiolase domain, extending from amino acids 1–404, and SCP2, which is located at the carboxyl terminus (Ossendorp et al. 1991). It is known from previous in vitro studies that SCPx has similar lipid transfer activity as SCP2 and that the substrate specificity of the SCPx thiolase shows a preference for straight medium chain acyl-CoA substrates and tetramethyl-branched 3-ketopristanoyl-CoA (Seedorf et al. 1994a; Wanders et al. 1997). Thus, the SCPx-associated thiolase differs from the initially identified peroxisomal thiolase that is assumed traditionally to play a major role in peroxisomal β-oxidation of most naturally occurring substrates, including bile acids and very long chain fatty-acids (VLCFA) (Hijikata et al. 1987; Schram et al. 1987).

In the present study, we investigated the biological function of *Scp2* by using gene targeting in mice. The phenotypic abnormalities of the *Scp2*(−/−) knockout (KO) mice revealed a profound impact of the gene disruption on the in vivo degradation of branched-chain fatty acyl-CoAs coming from the metabolism of tetramethyl-branched fatty acid phytanic acid. On the other hand, the serum concentrations of cholesterol, steroids, VLCFA, and long-chain fatty acids were not affected in *Scp2*(−/−) mice. This leads to our conclusion that one principal function of *Scp2* resides in the major peroxisomal pathway, which mediates the degradation of methyl-branched fatty acyl-CoA substrates in mice.

Results

To produce SCP2 and SCPx deficiency, we introduced a gene disruption at the exon 14 region of the gene (Fig. 1A). Transfection of the targeting vector into mouse E14 ES cells and subsequent positive–negative selection provided 182 clones. Southern blot analysis led to the identification of two correctly targeted clones (cl20, cl110) with only a single *neo* gene copy in the targeted locus (Fig. 1B). Injection of recombinant cl110 embryonic stem cells in blastocysts obtained from C57BL/6 donors, followed by embryo transfer into CD1 foster mothers generated five chimeras. Among these, we identified three transmitters that were crossed further with C57BL/6 mice.

Complete elimination of the *Scp2* gene function was confirmed by Northern blot experiments, showing a low-intensity signal derived from a truncated *Scp2* transcript in (−/−) mice that was ~150 nucleotides smaller than the corresponding transcript in normal C57BL/6 mice (Fig. 1C). When primers, flanking the region of the *Scp2* cDNA encoded by exon 14, were used for PCR amplification with reverse transcribed poly(A) RNA, isolated from (−/−) mice, a DNA fragment was obtained that again was ~150 bp smaller than normal. DNA sequencing of this DNA fragment revealed that the *Scp2* targeted allele led to abnormal splicing resulting in exon 14 skipping (Fig. 1D). The cDNA sequence predicted protein sequences of SCP2 and SCPx that were normal until position 22 and 427, respectively. Thereafter, the direct junction to the coding information of exon 15 resulted in a frame-shift, thereby creating a premature stop 18 codons downstream. Results from earlier site-directed mutagenesis studies lead to the conclusion that the predicted SCP2 variant should clearly lack any residual lipid transfer activity (Seedorf et al. 1994b). In contrast, the thiolase-like domain (residues 1–404) was preserved in the predicted SCPx variant, which may suggest the possibility of residual thiolase activity. However, because the carboxy-terminal peroxisomal targeting signal is absent, the variant should no longer be imported into peroxisomes and therefore, should be at least functionally inactive. Moreover, as shown in Figure 1E, liver extracts subjected to Western blot analyses developed with anti-SCP2 or anti-SCPx antibodies revealed complete absence of the two proteins in (−/−) mice. Homozygous transgenes also lacked the previously identified peroxisomal 44-kD thiolase-like peptide that was considered to result from proteolytic processing of SCPx (Seedorf et al. 1994a).

Genotyping showed that heterozygous (+/−) and homozygous (−/−) transgenes were viable. When kept under standard laboratory conditions, (−/−) mice developed normally and had no developmental abnormalities. We did not observe differences in the incidence of (+/+), (+/−), and (−/−) mice from the Mendelian distribution [27% (+/+), 52% (+/−), 21% (−/−), $n = 141$] indicating that the (−/−) allele did not affect the viability at 3–4 weeks of age. In addition, (−/−) males and females reached fertility at the normal age of ~6 weeks. Interbreeding between (−/−) males and (−/−) females gave rise to viable progeny. The litters were of comparable sizes as that found in (+/+) or (+/−) interbreeding. In 6- to 8-week-old males, testosterone and glucocorticoid concentrations were within the normal range. No differences between the two strains were also found for progesterone in nonpregnant females under baseline conditions. Whereas plasma insulin and cholesterol concentrations were normal, triglycerides were slightly higher and free fatty acid and glucose concentrations were moderately lower in (−/−) mice (Table 1).

All major tissues of the *Scp2*(−/−) mice were examined by light microscopy at various times after birth and compared with those of heterozygous and wild-type mice. Although the organ systems appeared morphologically normal, we observed more intense diaminobenzidine staining (DAB, stains specifically peroxisomes) in frozen liver sections from *Scp2*(−/−) mice than from controls (Fig. 2A). Enzyme activity levels of the peroxisomal marker catalase were 1.8-fold elevated in *Scp2*(−/−) liver. Likewise, peroxisomal palmitoyl-CoA oxidase (ACO), mitochondrial butyryl-CoA dehydrogenase, and total 3-ketooctanoyl-CoA thiolase activities were all two- to threefold higher in *Scp2*(−/−) mice than in controls (Fig. 2B). Whereas the hepatic levels of phospholipids were

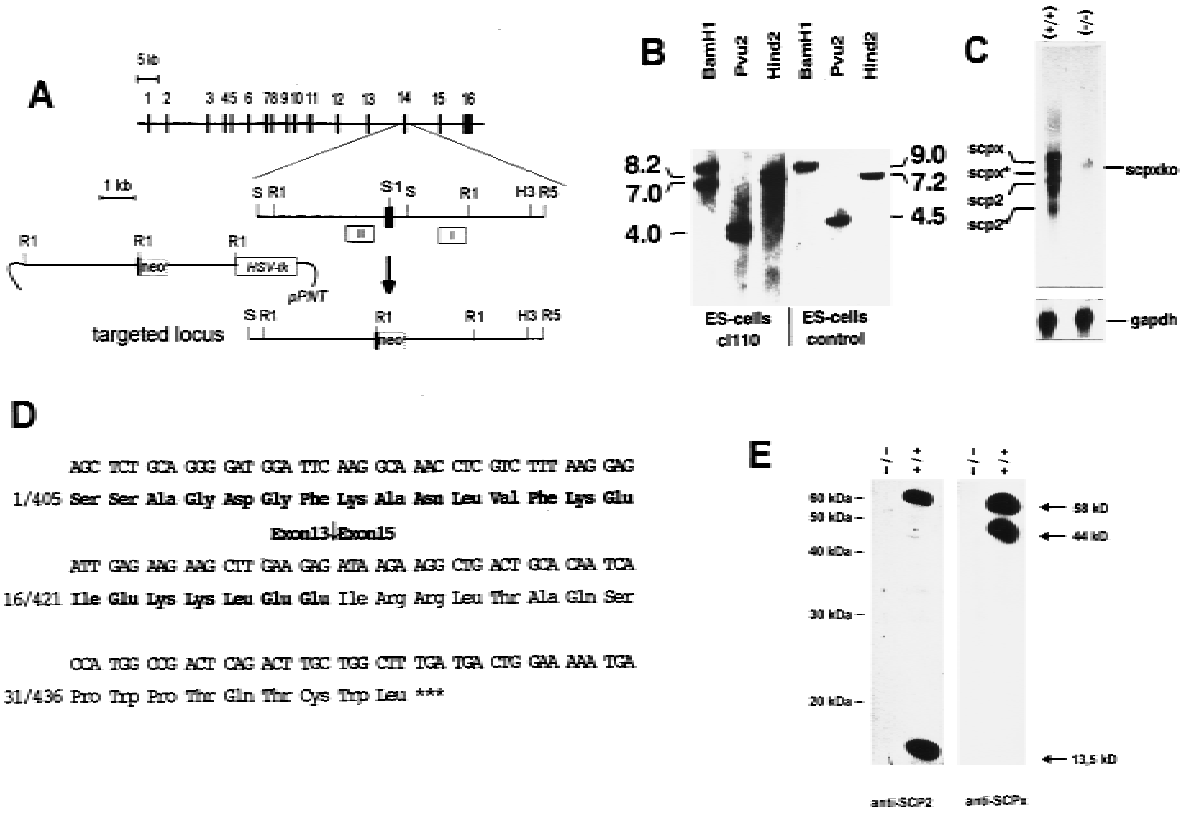

Figure 1. Targeted disruption of the murine *Scp2* gene by homologous recombination. (*A*) Structures of the *Scp2* gene (*top*), the exon 14 region of the locus, the *Scp2* targeting vector, and the targeted *Scp2* locus after homologous recombination (*bottom*). Only relevant restriction sites are shown: (H3) *Hin*dIII; (R1) *Eco*RI; (R5) *Eco*RV; (S) *Spe*I. The *Sal*I site (S1), shown in exon 14, was not present in the originally isolated genomic clone, but was introduced by site-directed mutagenesis to enable introduction of the *neo* gene cassette (see Materials and Methods for details). The *neo* gene and *HSV-tk* gene cassettes are indicated by boxes. The location of the vector pPNT is shown schematically by bend lines. The scale is indicated by the bars above the gene structure and the exon 14 region. The positions of the relevant probes are marked by open boxes. (*B*) Southern blot analysis with digested ES cell genomic DNA of a correctly targeted ES cell line (*left*, clone 110) and the parental cell line E14 (control), *right*. The sizes (in kb) of DNA fragments obtained after hybridization with probe I for the correctly targeted and the original allele are shown on either side. (*C*) Northern blot analysis of mouse liver RNA. Total RNA (20 μg) from wild-type (+/+) and *Scp2*(−/−) mice was used and hybridized to a labeled *Scp2* cDNA probe. The four normal *Scp2* transcripts of 2700 nucleotides (scpx), the major 1500-nucleotide *SCP2* transcript (scp2), and two minor alternatively polyadenylated transcripts (scp2*, 900 nucleotides; scpx*, 2200 nucleotides) are indicated. The sample from the homozygous *Scp2*(−/−) mouse provided a low-intensity signal of a transcript of ~2550 nucleotides (scpxko). As a control for identical sample loading the same Northern blot analysis was reprobed with a rat GADPH cDNA probe (*bottom*). (*D*) Direct DNA sequencing of the *Scp2* transcript from liver of (−/−) mice. The sequence is shown along with the translated amino acid sequence. The normal protein sequence is in boldface type. The shift of the normal reading frame that is caused by the direct junction of exons 13–15 is indicated by an arrow. The codon numbers (*left*) refer to the normal mouse SCP2 and SCPx cDNAs. (***) The location of the premature stop codon. (*E*) Western blot analysis of mouse liver proteins. The blots were developed with either polyclonal antibodies raised against recombinant rat SCP2, anti-SCP2, or antibodies raised against a recombinant 383-amino-acid amino-terminal peptide of SCPx (anti-SCPx). Arrows indicate bands corresponding to SCP2 (13.5 kD), SCPx (60 kD), and the 44-kD thiolase-like peptide (44-kD peptide). No specific reactivity was obtained with samples from (−/−) mice.

normal, cholesterol ester and triglyceride storage pools were markedly depleted in livers from *Scp2*(−/−) mice (Table 1). Intestinal lipid absorption was normal, as judged by monitoring intestinal uptake of radiolabeled cholesterol or palmitic acid. We also did not detect abnormal liver function, as indicated by normal GOT, GPT, γGT, and bilirubin serum levels (data not shown). Age- and sex-matched *Scp2*(−/−) and C57BL/6 mice had similar body weights, whereas food intake was significantly higher in *Scp2*(−/−) mice (256 ± 12.9 mg/day × grams of body weight) compared with controls (196 ± 10.7 mg/day × grams of body weight).

In addition to these biochemical abnormalities, the *Scp2* gene disruption had marked effects on hepatic gene expression. As shown in Figure 3, *Scp2*(−/−) mice showed increased expression of liver fatty acid-binding protein (L-FABP, fourfold), peroxisomal 3-ketoacyl-CoA thiolase (pTHIOL, three- to fourfold), mitochondrial 3-ketoacyl-CoA thiolase (mTHIOL, two- to threefold), ACO (twofold), and cholesterol-7α-hydroxylase (CYP7α, fourfold).

Table 1. *Laboratory values in* Scp2 *(–/–),* Scp 2 *(+/–) mice, and controls*

	Unit	*Scp2* (+/+)	*Scp2* (+/–)	*Scp2* (–/–)
Testosterone (serum)	nmoles/liter	3.0 ± 1.8	4.9 ± 2.2	2.0 ± 0.9
Progesterone (serum, ♀)	nmoles/liter	11.2 ± 6.9	12.5 ± 8.6	10.4 ± 3.0
Corticosteroids (serum)	ng/dl	188 ± 32	210 ± 44	204 ± 35
Insulin (serum)	ng/dl	161 ± 34	187 ± 40	207 ± 34
Cholesterol (serum)	mg/dl	71 ± 11	104 ± 20	66 ± 17
Triglycerides (serum)	mg/dl	89 ± 3	89 ± 16	105 ± 4*
Free fatty acids (serum)	mM	1.12 ± 0.09	1.08 ± 0.10	0.72 ± 0.04*
Glucose (serum)	mg/dl	116 ± 13	108 ± 7	81 ± 3
Phospholipids (liver)	mg/gram	20.5 ± 1.2	19.7 ± 2.4	19.3 ± 2.6
Cholesterol (liver)	mg/gram	3.2 ± 0.3	2.9 ± 0.4	2.9 ± 0.4
Cholesterol ester (liver)	mg/gram	0.50 ± 0.12	0.47 ± 0.09	0.25 ± 0.06*
Triglycerides (liver)	mg/gram	66.2 ± 8.5	41.7 ± 9.5*	32.8 ± 6.9*

Values represent means ±S.E.M.; (*) $P \leq 0.05$ (comparison to controls with the paired *t*-test; ($n \geq 5$). Progesterone was measured in nonpregnant 8- to 12-week-old females. All other values are from 8- to 12-week-old males.

In contrast, no effect was observed on the level of GAPDH, β-actin, and sterol-27-hydroxylase (CYP27) expression, whereas phosphoenolpyruvate carboxykinase (PEPCK) expression was down-regulated in the *Scp2*(–/–) group, which corresponded to mild hypoglycemia in that group (Fig. 3, Table 1).

Whereas we did not detect significant differences regarding the relative levels of the straight long chain saturated, monounsaturated, polyunsaturated, or VLCFAs (data not shown), phytanic acid was close to 10-fold elevated in (–/–) mice compared with controls (Table 2). Phytanic acid is a tetramethyl-branched fatty acid that is produced in heterotrophic organisms from plant-derived phytol (an isoprenoic alcohol esterified to ring IV of chlorophyll). Because neither phytanic acid nor phytol are synthesized de novo in mammals, phytanic acid serum concentrations depend on dietary intake of preformed phytanic acid or its precursor phytol, storage of phytanic acid in cellular neutral lipids, and the catabolic rate of phytanic acid (Steinberg 1995). Because only low amounts of free phytol (75 μg/gram) and phytanic acid (200 μg/gram) were present in the normal laboratory diet, we performed feeding experiments with semisynthetic diets supplemented with phytol. When *Scp2*(–/–) mice were exposed to a diet containing 5 mg/g of phytol for 7 days, the levels in serum of phytanic acid increased from 16 to 1163 μmoles/liter, whereas in *Scp2*(+/+) mice, it increased from 1.4 to 129 μmoles/liter (Table 2). Likewise, when we used a more natural high-fat diet (containing 15% coconut butter, which is a rich natural source of phytanic acid and phytol), phytanic acid plasma levels were more than tenfold higher in *Scp2*(–/–) mice compared with controls. In addition, elevated phytanic acid concentrations were also detected in sera from heterozygotes (Table 2).

We then exposed male mice of the two strains to phytol-enriched diets for 4 days, followed by a period of 10 days in which they were fed the standard low-phytol diet. In (+/+) mice, dietary intake of the phytol-enriched food induced an increase in serum phytanic acid concentrations up to 69 μmoles/liter (Fig. 4). After the diet change, the concentrations declined to 1.5 μmoles/liter within 2 days. In (–/–) mice phytanic acid reached a maximum of 354 μmoles/liter and declined to 36 μmoles/liter at day 10. Thereafter, phytanic acid continued to decline slowly, reaching 18 μmoles/liter at the end of the experiment. In contrast to (+/+) mice, who revealed a close to twofold transient increase with respect to liver catalase activities, the values remained close to twofold above normal in (–/–) mice throughout the experiment (Fig. 4).

Catabolism of phytanic acid proceeds by way of α-oxidation, yielding the (n – 1) lower homolog pristanic acid (C19:0), which is further catabolized by way of β-oxidation in peroxisomes (Singh et al. 1994; Singh and Poulos 1995; Steinberg 1995). To discriminate between defective phytanoyl-CoA α-oxidation and pristanoyl-CoA β-oxidation, we then quantified pristanic acid. However, pristanic acid could not be detected in sera from *Scp2*(+/+), *Scp2*(+/–), or *Scp2*(–/–) mice under normal conditions. Only after phytol enrichment of the diet, pristanic acid concentrations were two- to threefold higher in *Scp2*(–/–) mice than in the two other strains (Table 2). To investigate the block in phytol catabolism more specifically, we continued to analyze phytol metabolites in saponified liver lipid extracts by time-of-flight secondary-ion-mass-spectrometry (TOF-SIMS) (Fig. 5A). This method enabled us to detect a wider range of metabolites than could be identified by gas chromatography. Evaluation of the signal intensities of the relevant ions indicated accumulation of phytanic acid (six- to eightfold), Δ2,3-pristenic acid (four- to fivefold), 3-OH-pristanic acid (three- to fourfold), and pristanic acid (twofold) in (–/–) liver (Fig. 5C). Because model analyses with 3-ketoacyl acids indicated that they were not stable during the analysis (data not shown), 3-ketopristanic acid could not be measured directly. However, we looked for the product of the thiolytic cleavage of 3-ketopristanoyl-CoA, detected at 255.3 mu (corresponding to the $[M\text{-}H^+]^-$ ion of 4,8,12-trimethyltridecanoic acid; TMTDA). As expected for deficient thiolytic cleavage of 3-ketopristanoyl-CoA, the respective signal was found 70% re-

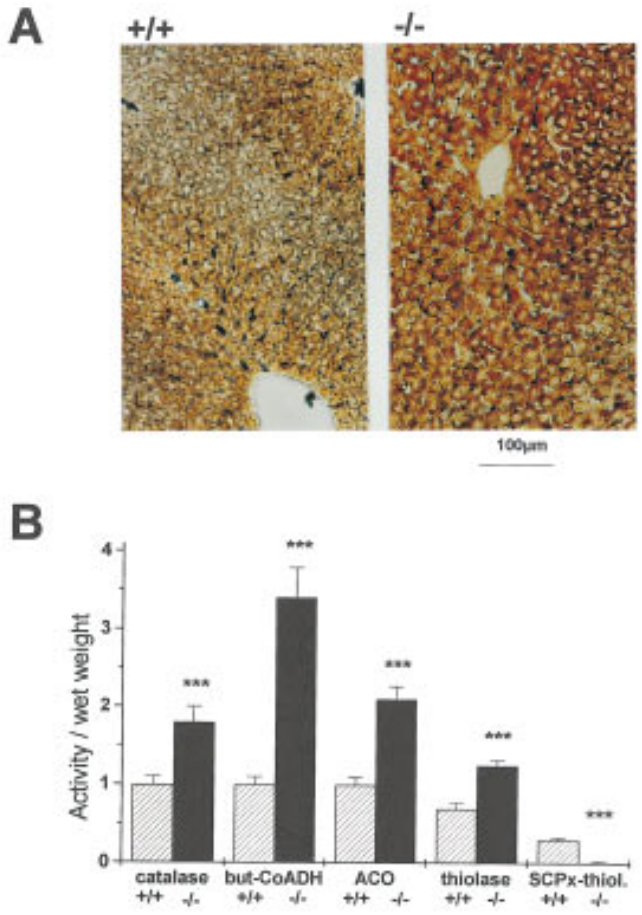

Figure 2. Peroxisomal proliferation and induction of β-oxidation in *Scp2*(−/−) mice. (*A*) Diaminobenzidine staining of liver sections. The bar indicates scale (*bottom*); the selected images are representative for five animals of each strain. (*B*) Enzyme activities (units/gram of wet weight) of catalase, mitochondrial butyryl-CoA dehydrogenase (but-CoADH), ACO, and 3-ketooctanoyl-CoA thiolase/(SCPx-thiol.) are shown. The activity of the SCPx thiolase was determined after immunoprecipitation with an antibody directed against the amino-terminal 383 amino acids of the protein. The columns represent ratios between *Scp2*(−/−) samples and controls ±S.D.; (***) paired *t*-test; (P) < 0.005.

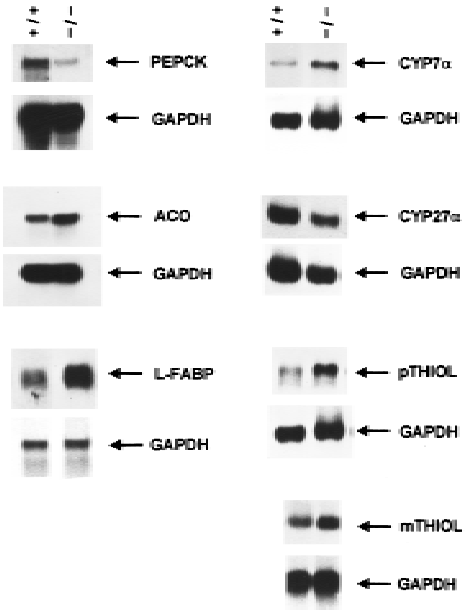

Figure 3. Altered gene expression in *Scp2*(−/−) mice. Northern blots of liver RNA were hybridized with probes derived from PEPCK, ACO, L-FABP, CYP7α, CYP27α, pTHIOL, and mTHIOL. As a control for identical sample loading, Northern blots were reprobed with a rat GADPH cDNA probe. The selected images are representative for at least five animals of each strain. The relative signal intensities were evaluated by laser densitometry and are given in the text.

pressed in *Scp2*(−/−) mice (Fig. 5B,C). Likewise, the signal of the next predicted downstream metabolite, 4,8,12-trimethyl-Δ2,3-tridecenoic acid (Δ2,3-TMTDA), was also close to threefold higher in controls than in the transgenic strain (Fig. 5B,C). In contrast, signals expected for phytol (detected as a negative ion at 293.5 mu) were barely detectable in all samples, suggesting that conversion of phytol to phytanic acid occurred with high efficiency in both strains of mice.

These data support the concept that phytol degradation is inhibited at a step downstream of phytanoyl-CoA α-oxidation. They are also in line with recent findings by Wanders et al. (1997) that purified recombinant rat SCPx protein exhibits high 3-keto-pristanoyl-CoA thiolase activity. On the other hand, the large accumulation of phytanic acid, which exceeded that of pristanic acid under these experimental conditions, pointed to a partial block also at an early step of phytanic acid breakdown. Because expression of phytanoyl-CoA hydroxylase was not downregulated in *Scp2*(−/−) mice (Fig. 6A), we hypothesized that SCP2 could function as an auxiliary factor in phytanic acid oxidation (i.e., by acting as a peroxisomal bind-

Table 2. *Phytanic and pristanic acid in sera from* Scp2 *(+/+),* Scp 2 *(+/−), and* Scp2 *(−/−) mice*

	Diet	*Scp2*(+/+)	*Scp2*(+/−)	*Scp2*(−/−)
Phytanic acid	chow	1.4 ± 0.4	4.8 ± 2.6*	16 ± 3*
	high fat	16 ± 6	33 ± 6*	152 ± 11*
	5 mg/gram phytol	129 ± 26	313 ± 44*	1163 ± 367*
Pristanic acid	chow	< 0.5	< 0.5	< 0.5
	high fat	< 0.5	< 0.5	< 0.5
	5 mg/gram phytol	15 ± 8	17 ± 6	47 ± 26

Results are expressed in μmoles/liters as mean ±S.D. ($n \geq 5$); (*) paired *t*-test, $P < 0.05$. (< 0.5 μmole/liter) Not detectable. Quantitation and identification was performed by gas chromatography of the carboxy-methylated derivatives by comparison with appropriate standards. Details regarding the various diets are described in Materials and Methods.

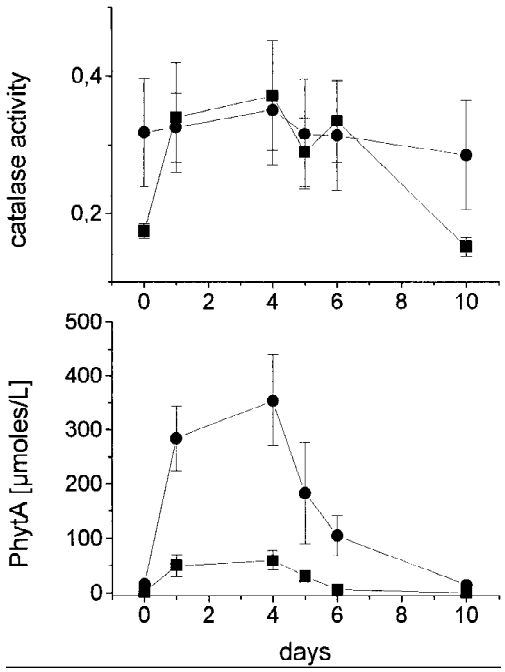

Figure 4. Phytanic acid levels and liver catalase activities in *Scp2*(−/−) mice (■) and controls (●). Six- to 8-week-old male mice were fed a standard chow diet supplemented with 2.5 mg/gram of phytol for 4 days, followed by the standard diet without phytol supplementation. Phytanic acid concentrations in serum ($n = 3$) are given in µmoles/liter (*top*); catalase activities were determined in liver and are expressed as arbitrary units/gram wet weight (*bottom*).

ing protein or substrate carrier). To evaluate this possibility, we determined binding affinities of phytanic acid, pristanic acid, phytanoyl-CoA, pristanoyl-CoA, and cholesterol of recombinant rat SCP2. We used a fluorescence resonance energy transfer (FRET) competition assay. In this assay, competitive inhibition of the binding of pyrenyl-dodecanoic acid to recombinant SCP2 by the nonlabeled substrates was monitored using FRET between the single tryptophan residue of SCP2 (donor) and the pyrene acceptor of the labeled fatty acid. The results showed that the recombinant SCP2 protein had a high affinity for phytanoyl-CoA binding (K_d, 250 nM), whereas the affinities for binding of pristanoyl-CoA, pristanic acid, and phytanic acid were considerably lower (Fig. 6B). In addition, we found that the affinity of the interaction between phytanoyl-CoA and SCP2 was severalfold higher than that of cholesterol (which led to the traditional name sterol carrier protein) (Fig. 6B).

Diets containing up to 2.5 mg/gram of phytol were tolerated rather well in *Scp2*(−/−) mice. Although body weights declined slowly by up to 25% within 6 weeks, we noticed no signs of toxicity. Apart from their skinny appearance, *Scp2*(−/−) mice looked healthy, they remained active, had no signs of neurological abnormalities, and dietary intake was high until the end of the experiment at 6 weeks. Mobilization of body mass was maximal within the first few days and occurred in the absence of significant differences in food intake (Fig. 7A). In parallel, *Scp2*(−/−) mice developed more pronounced hypolipidemia than controls (Fig. 7B). Higher phytol enrichment of the diet (5 mg/gram) led to much more severe abnormalities. Already beginning with the first day, (−/−) mice lost body weight extensively, which declined rapidly until they reached close to 60% of their starting weights at the end of the second week (Fig. 7A), when we noticed an unhealthy appearance, inactivity, reduced muscle tone, ataxia, and peripheral neuropathy (uncoordinated movements, unsteady gait, and trembling). Already after 1 week, *Scp2*(−/−) mice showed pronounced decreases of lipid and glucose levels in serum and almost complete absence of fat tissue (Fig. 7C). The values obtained in serum for GPT, GOT, and alkaline phosphatase were severalfold elevated and liver histology indicated pronounced liver disease. All *Scp2*(−/−) mice died in the third week, presumably because the extensive neurological disturbances progressively disabled their food intake. In contrast, controls tolerated both diets well until the end of the experiment (6 weeks). When 5 mg/gram of phytol were added to the diet, we observed only a moderate decrease in body weight (−15%), mild hypolipidemia, and hypoglycemia, and moderately elevated serum GPT levels without morphological signs of liver disease or reduced food intake. In contrast, supplementation of the diet with >50 mg of phytol per gram of food led to a similar range of abnormalities and premature death in controls, as could be observed with 5 mg/gram in the transgenic strain (data not shown).

Discussion

In the present study, we used gene targeting to investigate the function of *Scp2* in mice. We were interested in this approach because there is no human inherited disease known that results from *Scp2* mutations and the great manifold of in vitro studies, which were performed during the past two decades, have not led to a convincing functional conclusion. Because the defective allele contained only one correctly targeted *neo* gene and the recombinant genetic abnormality based on a specific molecular mechanism, associated with exon 14 skipping and thus abnormal splicing of *Scp2* transcripts, it is highly unlikely that the abnormalities are attributable to a linked or incidental genetic defect rather than to the *Scp2* gene disruption itself. Moreover, also heterozygous mice had elevated phytanic acid concentrations, indicating that this intermediate quantitative phenotype depended on the gene dosage. Although the gene disruption did not completely eliminate synthesis of *Scp2* transcripts, the abnormal RNAs were barely detectable and encode truncated SCP2 and SCPx peptides that should be functionally inactive and were not detected in *Scp2*(−/−) mice. We conclude that the targeted allele is associated with complete SCP2 and SCPx deficiency and thus, behaves like a null allele.

We believe our data demonstrate convincingly that abnormal phytol catabolism is a primary effect of the gene disruption. Phytol is a natural tetramethyl-branched acyl

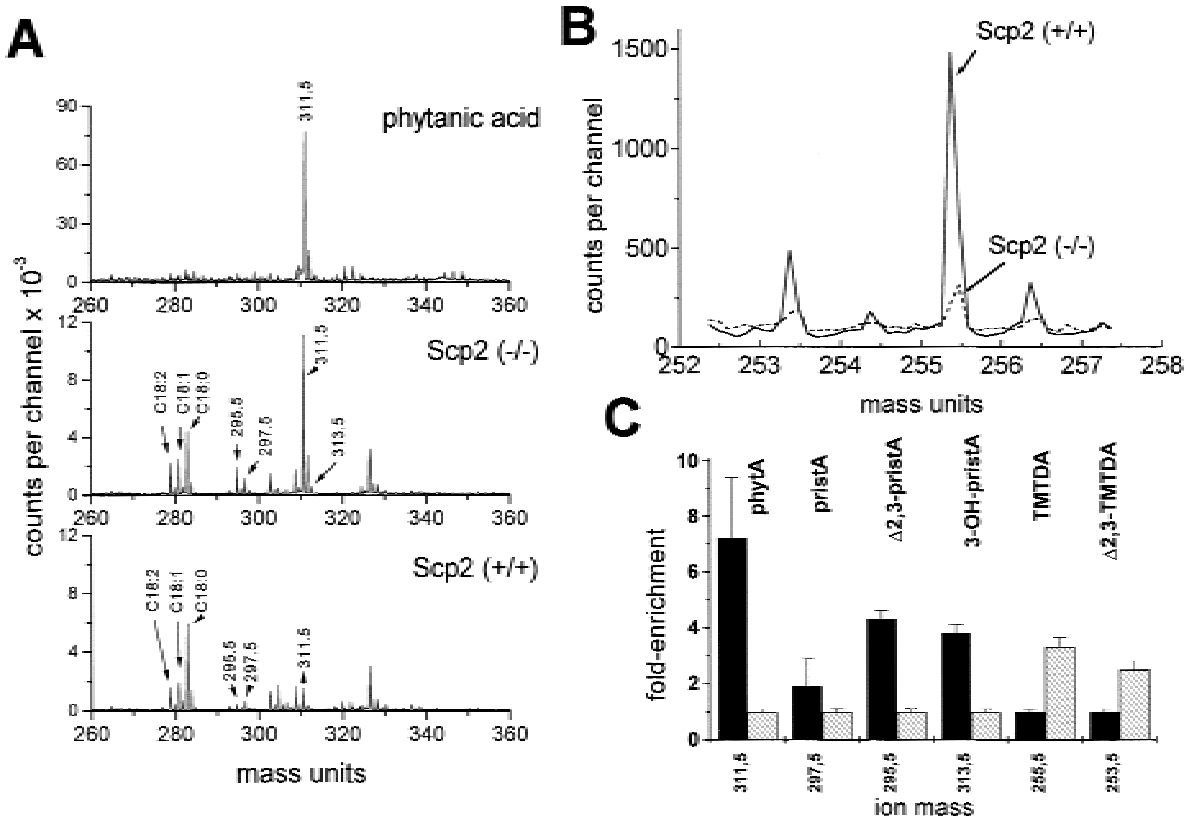

Figure 5. Defective phytol catabolism in *Scp2*(−/−) mice. (*A*) Detection of phytanic acid and its catabolic metabolites in the liver by TOF-SIMS analysis. (*Top*) Mass spectrum of the phytanic acid standard (1 pg). The compound was detected as a negative ion at 311.5 mu, representing the $[M\text{-}H^+]^-$ ion. (*Middle*) Lipid extracts were prepared from liver of *Scp2*(−/−) mice and subjected to TOF-SIMS analysis using identical conditions as for the standard. Arrows point to phytanic acid (311.5 mu), and the expected signals for Δ2,3-pristenic acid (295.5 mu), pristanic acid (297.5 mu), and 3-OH-pristanic acid (313.5 mu). The signals obtained for the 18 carbon atoms straight chain fatty acids C18:0, C18:1, and C18:2 are also marked. (*Bottom*) The same analysis with a liver sample from an *Scp2*(+/+) mouse. The images are representative for five mice of each genotype and both sexes. (*B*) Monitoring of ions corresponding to the predicted products of thiolase-mediated 3-ketopristanoyl-CoA cleavage (at 255.5 mu, TMTDA; at 253.5 mu, Δ2,3-TMTDA). (*C*) Quantitative evaluation of the signal intensities based on five mice of each strain and sex. The columns indicate mean values of fold difference between either (−/−) mice or controls; ±S.E.M.. Black bars (−/−); hatched bars (+/+).

alcohol, originating from the isoprenoic side chain esterified to ring IV of chlorophyll. In humans, the daily dietary intake of phytol and its product phytanic acid is in the order of 100 mg/day, but intake varies greatly depending on dietary habits (Steinberg 1995). As illustrated in Figure 8, normal catabolism starts with the conversion of phytol to phytanic acid, followed by activation to phytanoyl-CoA in the cytoplasm. Phytanoyl-CoA is then imported into peroxisomes followed by α-oxidation, which involves hydroxylation at the α-carbon position by phytanoyl-CoA hydroxylase (PHYH). Subsequently, 2-OH-phytanoyl-CoA is converted to pristanic acid and formyl-CoA (Wanders et al. 1994; Croes et al. 1997). Whereas formyl-CoA is further catabolized in mitochondria, pristanic acid is activated to pristanoyl-CoA, which is then subject to six cycles of peroxisomal β-oxidation. The intermediates of the first cycle are Δ2,3-pristenoyl-CoA (produced by pristanoyl-CoA oxidase), 3-OH-pristanoyl-CoA, and 3-ketopristanoyl-CoA (produced by a peroxisomal bifunctional enzyme). Finally, 3-ketopristanoyl-CoA is substrate for thiolytic cleavage, catalyzed by a 3-ketopristanoyl-CoA thiolase, which yields the (n-3) lower homolog of pristanoyl-CoA (4,8,12-trimethyltridecanoyl-CoA) and propionyl-CoA (for review, see Steinberg 1995). Although studies on mice are not available, it now appears that this pathway operates in a similar way in rats and humans (Watkins et al. 1994; Singh and Poulos 1995).

We detected pronounced accumulation of phytanic acid in *Scp2*(−/−) mice, which exceeded that of pristanic acid and the downstream catabolic intermediates by severalfold. This may be explained by inhibition of initial phytanic acid activation, phytanoyl-CoA import into peroxisomes, or phytanoyl-CoA α-hydroxylation. Abnormal activation was unlikely because recent studies demonstrated convincingly that phytanoyl-CoA ligation is mediated by a common long chain fatty acyl-CoA ligase (Watkins et al. 1996), whereas metabolism of long straight chain fatty acids was apparently not affected by the gene disruption. Because *PHYH* was expressed nor-

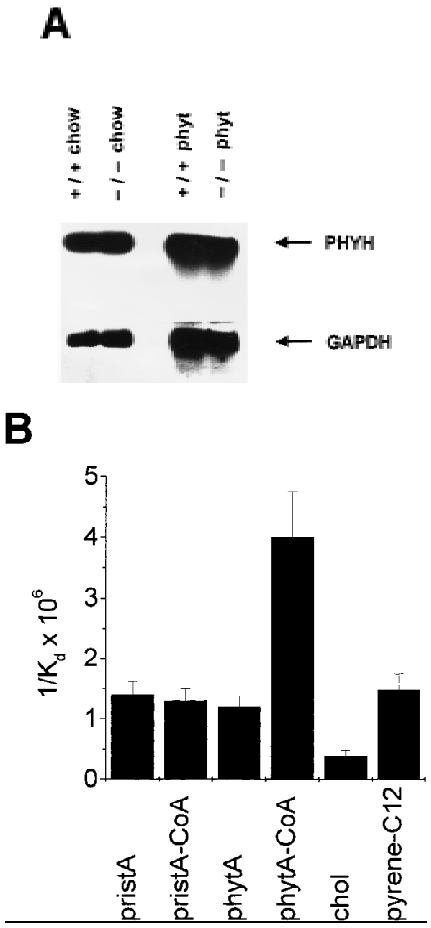

Figure 6. Expression of phytanoyl-CoA hydroxylase in *Scp2*(−/−) mice. Northern blots of liver RNA were hybridized with a labeled *PYHH* cDNA probe (*A*). Specific phytanoyl-CoA-binding activity of recombinant rat SCP2 (*B*). The columns represent means of $1/K_d$ ± S.D. of five independent determinations.

mally in *Scp2*(−/−) mice, we also excluded secondary down-regulation of *PHYH* expression. On the basis of these considerations, we hypothesized that the lipid carrier function of SCP2 may be involved in peroxisomal phytanoyl-CoA uptake (i.e., by acting as phytanoyl-CoA binding protein). The analysis, which was performed with a very specific FRET competition assay on the purified recombinant rat protein, revealed a much higher affinity for binding of phytanoyl-CoA than of pristanoyl-CoA, phytanic acid, pristanic acid, or cholesterol. In addition, the K_d value was within a physiologically meaningful range (250 nM), thus supporting the postulated indirect role of SCP2 in peroxisomal phytanoyl-CoA uptake.

Impaired phytanoyl-CoA import into peroxisomes would lead to the expectation that the production of downstream intermediates, which are generated in peroxisomes from phytanoyl-CoA, should be repressed in *Scp2*(−/−) mice. In contrast, evaluation of TOF-SIMS signals, which corresponded to these intermediates, indicated even higher concentrations than in controls after challenging mice with high dosages of dietary phytol. Although the twofold increase in pristanic acid did not reach statistical significance, accumulation of Δ2,3-pristenic acid (four- to fivefold) and 3-OH-pristanic acid (three- to fourfold) was highly significant. In contrast, 3-ketopristanic acid was not stable enough to withstand alkaline extraction and subsequent TOF-SIMS or GC-MS analyses. We could, however, detect a very significant 70% repression of the signals produced by the downstream products of the 3-ketopristanoyl-CoA thiolase reaction in *Scp2*(−/−) mice (4,8,12-trimethyltridecanoic acid and 4,8,12-trimethyl-Δ2,3-tridecenoic acid). Together with enrichment of upstream intermediates in pristanic acid β-oxidation, the latter result supported very clearly inhibition at the level of 3-ketopristanoyl-CoA cleavage. These in vivo data corresponded to recent studies, which demonstrated high specific activity of recombinant rat SCPx to catalyze the thiolytic cleavage of 3-ketopristanoyl-CoA in vitro (Wanders et al. 1997). Thus, our data appear to indicate a dual effect of the gene disruption, consisting of reduced peroxisomal phytanoyl-CoA import combined with defective thiolytic cleavage of 3-ketopristanoyl-CoA. Whereas the first effect seems to relate to the phytanoyl-CoA carrier function of SCP2, the second may reflect the enzymatic activity associated with SCPx. This hypothesis appears very compelling, because it may clarify why evolution has established a molecular basis for coexpression of the two *Scp2*-encoded functions by fusing two originally separated SCP2 and thiolase genes into one common transcriptional unit. The fused gene is present in all vertebrates and could be traced back to *Drosophila melanogaster* (GenBank accession no. X97685). In contrast, two separated genes were identified in *Caenorhabditis elegans* and several yeast species (Pfeifer et al. 1993b; Bunya et al. 1997). Interestingly, an ancient precursor of SCP2 could be identified even in the primitive methanogenic archaeon *Methanococcus jannaschii* (Bult et al. 1996), in whom methyl-branched fatty acids play a prominent role.

As expected, (−/−) mice revealed a higher increase of phytanic acid concentrations than controls, when we challenged the two strains of mice transiently with phytol-enriched diets. However, after switching to the low phytol diet, *Scp2*(−/−) mice eliminated phytanic acid from the bloodstream at a surprisingly high initial rate, followed by a much slower decline after 6 days. Because it is known from studies on patients with Refsum disease that excess phytanic acid can be taken up by cells and stored in triglycerides (Steinberg 1995), the high initial rate most likely reflected cellular uptake and storage rather than high residual activity for phytanic acid breakdown. On the basis of the slow rate of the late decline, we calculated this activity to ~10%. This was in line with our other findings—10-fold higher steady-state concentrations of phytanic acid and ~10-fold increased phytol toxicity. However, whether the residual activity is attributable to compensatory up-regulation of peroxisomal straight chain β-oxidation, the presence in our model of the SCP2-like activity associated with the 80-kD precursor of 17β-hydroxysteroid dehydrogenase type

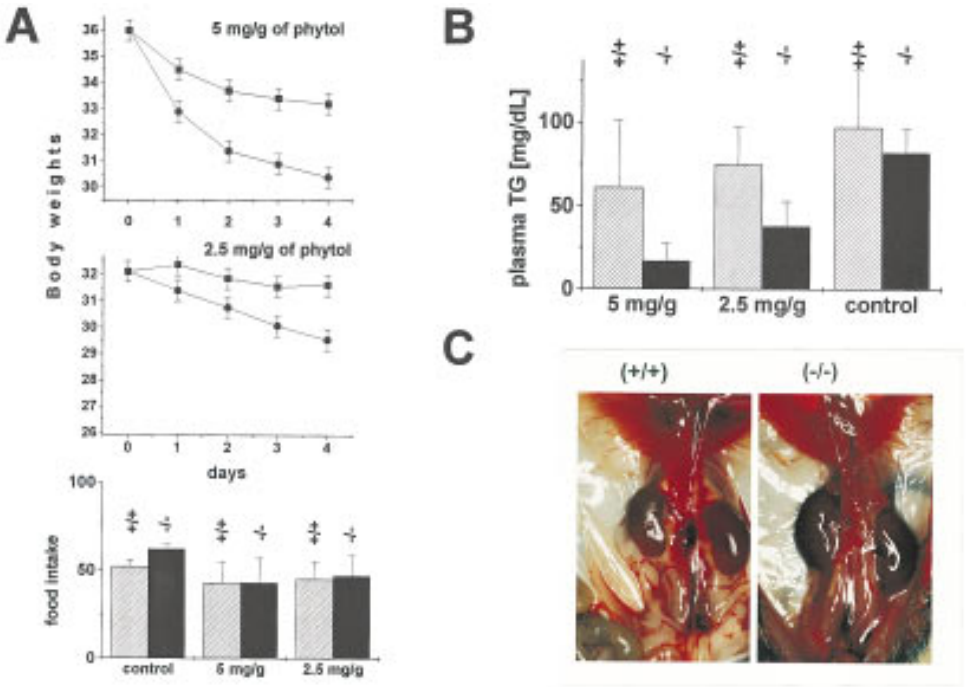

Figure 7. Phenotypic abnormalities in *Scp2*(–/–) mice after dietary phytol enrichment. (*A*) Six- to 8-week-old male mice ($n = 5$ in each group) were fed the standard chow diet (control) or the same diet supplemented with 2.5 or 5 mg/gram of phytol for up to 6 weeks. Body weights (*top*) and food intake (*bottom*, given as grams of food consumed in the 4-day period) were monitored daily. Results were obtained for the first 4 days, when decline of body weight was maximal. When *Scp2*(–/–) mice were fed the diet containing 5 mg/gram of phytol, they continued to mobilize body mass until they reached close to 60% of their starting weights. In the third week, they developed neuropathy, reduced their food intake, and died. (*B*) Serum triglyceride concentrations in the six experimental groups. The columns represent means ± S.D.. (*C*) Abdominal tissues in (+/+) (*left*) and (–/–) mice (*right*) after 10 days on the 5 mg/gram phytol diet. Note the normal appearance of the kidneys but hyperplastic and dark structures of the adrenal glands. In addition, lack of virtually any fat tissue, which is prominent in the (+/+) mouse, is evident in the (–/–) mouse. The abnormalities developed in the absence of significant reductions in food intake.

IV (Leenders et al. 1996), or an alternative pathway for phytanic acid oxidation, cannot be decided from our data.

Baum et al. (1997) reported that overexpression of SCP2 in rat hepatoma cells inhibited cholesterol esterification and HDL secretion, whereas plasma membrane cholesterol was significantly increased. In addition, Puglielli et al. (1995) showed that treatment of human skin fibroblasts with SCP2 anti-sense oligonucleotides led to inhibition of cholesterol net transfer to the plasma membrane. In view of these results, we found it surprising that *Scp2*(–/–) mice had significantly lower hepatic cholesterol ester storage than controls. Because the gene disruption also lowered free fatty acid and triglyceride concentrations very effectively, our results seem to indicate decreased availability of fatty acids for intracellular lipid esterification rather than a specific abnormality in cytosolic free cholesterol trafficking. It appeared interesting to us that hepatic hypolipidemia was associated with peroxisome proliferation and induction of peroxisomal and mitochondrial fatty acid β-oxidation in *Scp2*(–/–) mice. As is known from treatment of rodents with fibrates, induction of β-oxidation and peroxisome proliferation can lead to fatty acid hypermetabolism and hypolipidemia (for review, see Lemberger et al. 1996). The signals mediating peroxisome proliferation and modulation of gene expression in *Scp2*(–/–) mice are currently unknown. One possibility consists of a direct or indirect effect of accumulating phytol metabolites on nuclear signal transduction pathways (i.e., the peroxisome proliferator activated receptor PPARα being the most likely candidate in this respect).

Earlier studies provided several lines of indirect evidence that appear to support a role for SCP2 in adrenal and ovarian steroidogenesis (Pfeifer et al. 1993a). SCP2 is abundant in steroidogenic glands and trophic hormones stimulate steroidogenesis along with SCP2 gene expression (Trzeciak et al. 1987; Rennert et al. 1991). In addition, SCP2 enhanced the movement of cholesterol between vesicles and isolated mitochondria in vitro, which corresponded to increased pregnenolone synthesis in the in vitro system (Chanderbhan et al. 1982; Xu et al. 1991). Moreover, overexpression of SCP2 in COS cells engineered to produce progestins increased steroid formation (Yamamoto et al. 1991). On the other hand, no correlation existed between SCP2 expression and side chain cleavage activity in a variety of human tissue specimen (Yanase et al. 1996) and, a priori, it is not very clear how a peroxisomal protein would stimulate the net transfer of free cholesterol to mitochondria directly. So far, the phenotypic characterization of the *Scp2*(–/–) mouse has not provided any convincing evidence for a role of SCP2 in steroidogenesis in vivo. The absence of developmental abnormalities or salt wasting and the fact that (–/–) mice had no abnormalities affecting fertility, seemed to exclude an obligatory role of SCP2 in general steroidogenesis. This was in line with normal adrenal morphology and normal plasma concentrations of testosterone, progesterone, and glucocorticoids. On the other hand, a more subtle defect may be masked by compensatory mechanisms or depend on appropriate stress conditions.

In summary, the current phenotypic characterization of the *Scp2*(–/–) KO mouse model did not provide immediate convincing evidence for an obligatory role of

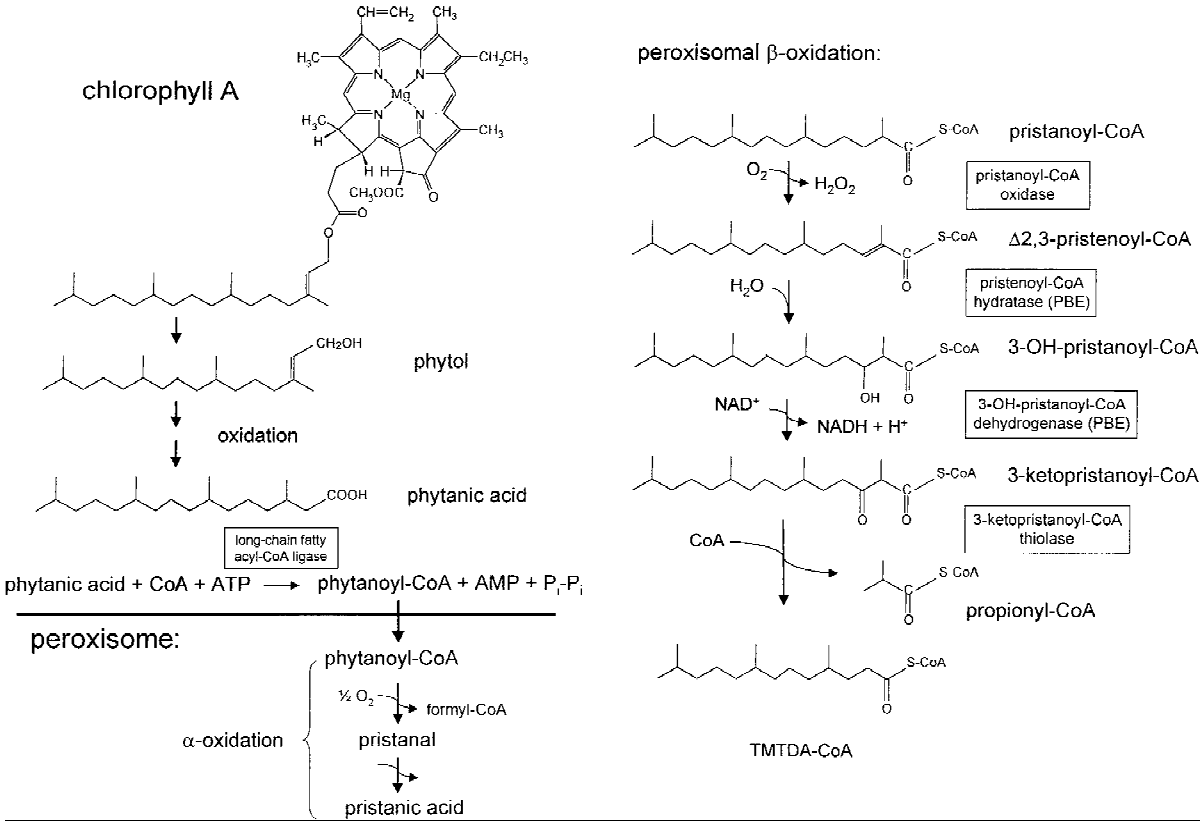

Figure 8. Schematic representation of mammalian phytol metabolism. Phytanic acid (3,7,11,15-tetramethylhexadecanoic acid) results either directly from the diet or from oxidation of dietary phytol. Note that phytanic acid must be decarboxylated to pristanic acid before entering peroxisomal β-oxidation, because the β-carbon atom is blocked by the 3-methyl group. Presumed intermediates of α-oxidation are 2-OH-phytanoyl-CoA and pristanal, but the precise cofactor requirements are currently unknown. Enoyl-CoA hydratase/3-OH-acyl-CoA dehydrogenase: peroxisomal bifunctional enzyme (PBE).

this gene in intracellular cholesterol trafficking. Instead, our data indicate that the two gene products SCP2 and SCPx cooperate in peroxisomal oxidation of certain naturally occurring tetramethyl-branched fatty acyl-CoAs in mice. Thus, the *Scp2* gene is somewhat reminiscent of a bacterial operon, in which distinct functions that act in the same metabolic pathway are combined in a common transcriptional unit. This role is consistent with its genetic organization, the well-established peroxisomal localization of SCP2 and SCPx (Keller et al. 1989; Ossendorp and Wirtz 1993), the ability of SCP2 to bind phytanoyl-CoA in vitro, high 3-ketopristanoyl-CoA thiolase activity of the SCPx protein (Wanders et al. 1997), and the expression pattern that correlates with lipid uptake of cells and thus phytanic acid exposition (Ossendorp et al. 1991; Seedorf and Assmann 1991; Yamamoto et al. 1991; Hirai et al. 1994; McLean et al. 1995).

Materials and methods

Construction of the targeting vector

Scp2 genomic sequences were isolated from a λ-Fix mouse genomic library (provided by Stratagene, Heidelberg, Germany) made of leukocyte DNA from mouse strain 129/SV. The basic fragment of the targeting construct was a 7.7-kb genomic *Eco*RI fragment containing exon 14 as the only *Scp2* coding sequences. Because exon 14 did not contain an appropriate restriction site, a 1.8-kb *Hin*dIII–*Spe*I fragment including the exon and flanking intron sequences was first subcloned in pBluescript SK$^-$ and a *Sal*I site was introduced into exon 14 by PCR-mediated site-directed mutagenesis (wild-type sequence, 5′-GTGAAG; mutated sequence, 5′-GTCGACG). The mutated fragment was reintroduced into the original 7.7-kb *Eco*RI fragment and this fragment was then cloned in the *Eco*RI site of a modified pBluescript vector (lacking the restriction sites *Hin*dII, *Hin*dIII, *Sal*I, *Eco*RV, and *Spe*I from its multicloning site). Double digestion of this vector with *Sal*I and *Spe*I released a 250-bp DNA fragment containing 110 bp of the exon 14 3′-part and 140 bp of flanking intron 14 sequences. After treatment with Klenow enzyme, the 1.2-kb *Xho*I–*Hin*dII fragment containing the *neo* gene cassette from the vector pMC1*neo*Poly(A) was blunt-end cloned into the double digested vector, thereby replacing the exon 14–intron 14 region of the *Scp2* gene by the *neo* gene cassette. The 8.7-kb *Not*I–*Kpn*I fragment from the resulting vector was cloned into the vector pPNT that was linearized by *Not*I digestion and used for transfection of ES cells.

Culturing and electroporation of ES cells

Experiments were carried out with the strain 129/Ola-derived ES cell line E14 (Hooper et al. 1987) provided by N. Maeda

(University of North Carolina). The cells were cultured on G418-resistant mouse embryonic fibroblast feeder layers as described earlier (Zhang et al. 1992). ES cells (3×10^7 cells) were resuspended in 0.5 ml of PBS containing 25 µg of linearized targeting vector and electroporated for 1 sec with a Bio-Rad GenePulser at 200 µF and 300 V per 0.4 cm. Cells were then seeded on eight Petri dishes (diameter, 10 cm) coated with fibroblast feeder layers. Selection with G418 (200 µg/ml, GIBCO) was started after 1 day and selection with gancyclovir (2 µM) after 2 days. After 12 days of growth, individual colonies were picked. Each colony was scraped from the plate with a sterile glass capillary and transferred to a 24-multiwell plate coated with fibroblast feeder layers and containing 1 ml of growth medium supplemented with 200 µg/ml G418, 2 µM Gancyclovir, and 100 U/ml of penicillin and streptomycin. After 2 days, each colony was disrupted with trypsin [0.025% wt/vol]. Four to 8 days later, the cells were trypsinized again and ~90 % of the cells were removed for DNA isolation. The remaining cells were transferred into new coated multiwell plates and after the cells were grown to a final density of 1.5×10^6 to 2.5×10^6 cells per well, they were frozen in growth medium containing 10% dimethylsulfoxide.

DNA analysis of ES cells and mice

Cells were lysed in 200 µl of 1% SDS, 25 µg of proteinase K per milliliter for 12–16 hr at 55°C. Thereafter, 100 µl of saturated NaCl was added, mixed, and centrifuged in an Eppendorf benchtop centrifuge at maximal speed for 15 min. The DNA was ethanol precipitated from the supernatant and dissolved in 25 µl of Tris-EDTA buffer (TE). Eight microliters of this solution was digested with the appropriate restriction enzyme, fractionated in 0.8% agarose gels and transferred to nitrocellulose (0.1-µm pore size; Schleicher & Schuell). Hybridization was performed as described (Raabe et al. 1996) with final washes in 0.1× SSC, 0.1% (wt/vol) SDS at 65°C for 30 min. DNA for genotype analysis was isolated from mouse tail tips as described by Laird et al. (1991).

RNA and Western blot analyses, PCR, and DNA sequencing

Total RNA was isolated from mouse tissues with the guandinium–thiocyanate–phenol–chloroform extraction procedure (Chomczynski and Sacchi 1987) followed by selection of poly(A) RNA on oligo(dT) cellulose. Northern blots were hybridized with digoxigenin-labeled probes prepared by random priming using a commercially available kit (Boehringer, Mannheim, Germany). All probes were obtained from a mouse liver cDNA library by PCR amplification with appropriate primers. Quantification was carried out relative to expression of GAPDH, detected with a probe derived from a 1.3-kb *Pst*I fragment from pGAPDH (Fort et al. 1985) containing rat glyceraldehyde-3-phosphate dehydrogenase cDNA, the probe for detection of *Scp2* expression was a 0.45-kb *Pst*I fragment from pBS-mSCPx containing mouse sterol carrier protein X cDNA (Seedorf et al. 1993). The membranes were rinsed twice in 0.1% SDS, 2× SSC at room temperature and then twice in 1% SDS, 0.5× SSC at 68°C for 15 min. Bands were visualized using the chemiluminescence substrate CDP-Star (Tropix-Serva, Heidelberg, Germany). DNA sequencing was performed on an automated laser fluorescence DNA sequencer (Pharmacia, Upsala, Sweden) according to the instruction manual of the supplier. Detection of SCP2-related peptides by Western blot analysis was described earlier (Seedorf et al. 1994a).

Dietary intervention studies, and histological and anatomical analyses

In most experiments, 6- to 24-week-old male mice were used. However, the defect in phytol catabolism was confirmed to be present also in a group of 25 female mice. Mice were fed a standard chow diet [(Altrumin, Hanover, Germany) containing 0.8 mg/gram (wt/wt) of various sterols, mainly cholesterol and β-sitosterol, 0.075 mg/gram (wt/wt) of nonesterified phytol and 0.2 mg/gram (wt/wt) of phytanic acid] and water of pH 3.4–3.6 ad libitum. The high fat diet consisted of standard chow supplemented with 1% cholesterol, 15% coconut butter, and 0.5% cholate. Phytol-enriched diets were prepared from these diets by adding 1–50 mg/gram (wt/wt) of phytol (Aldrich, St. Louis, MO). Animals were kept individually, and food intake and body weights were monitored daily. Tissues were dissected routinely between 9 and 10 a.m. (to exclude variations that might be attributable to circadian regulation) after lethal anesthesia with avertin (Sigma). Tissues were fixed in phosphate-buffered formaldehyde (pH 7.2) embedded in paraffin, sectioned at 5 µm, and stained with appropriate stains.

Binding of fatty acids to SCP2

Binding constants for the interaction between recombinant rat SCP2 and phytanic acid, phytanoyl-CoA, pristanic acid, or pristanoyl-CoA were determined by competing bound pyrene-labeled dodecanoic acid with the nonlabeled substrates. Binding of pyrenyl-dodecanoic acid was monitored using FRET between the single tryptophan residue of SCP2 (donor) and the pyrene acceptor of the labeled fatty acid. The signals were corrected for direct excitation of pyrene at 280 nm. The competitor-induced decrease in sensitized emission was fitted to a binding equation derived from the rate equations of the relevant bimolar binding reactions.

Analytical techniques, serum chemistry, and statistical analyses

Serum samples were taken by orbital bleeding or heart puncture. Serum chemistry was performed by routine clinical tests on a Hitachi 747 analyzer with sample volumes of 0.15 ml. Hormones were measured using commercially available radioimmunoassay kits (Diagnostic Products Corp., Los Angeles, CA). Fatty acids and phytanic and pristanic acid in serum were measured by gas chromatography. Identification was achieved with appropriate standards and verified by mass spectrometry as described earlier. Analyses in the liver of phytol metabolites were performed by TOF-SIMS as described earlier (Seedorf et al. 1995). All measurements were performed at least in triplicates. Statistical analyses were performed with the paired *t*-test. Values of $P \leq 0.05$ were considered statistically significant.

Acknowledgments

We thank B. Glass, K. Kluckman, and D. Lee for expert technical assistance. Dr. R. Voss assisted in standardizing TOF-SIMS-based metabolite quantitation. This work was supported by grants from the Deutsche Forschungsgemeinschaft (Se 459/2-2), the Interdisziplinäres Klinisches Forschungszentrum (Project A4) of the Medical Faculty, University of Münster, the Boehringer Ingelheim Stiftung, Bristol Myers Squibb, and the Bayer AG.

The publication costs of this article were defrayed in part by payment of page charges. This article must therefore be hereby marked "advertisement" in accordance with 18 USC section 1734 solely to indicate this fact.

References

Baum, C.L., E.J. Reschly, A.K. Gayen, M.E. Groh, and K. Schadick. 1997. Sterol carrier protein-2 overexpression enhances sterol cycling and inhibits cholesterol ester synthesis and high density lipoprotein cholesterol secretion. *J. Biol. Chem.* **272:** 6490–6498.

Bloj, B. and D.B. Zilversmit. 1977. Rat liver proteins capable of transferring phosphatidylethanolamine. Purification and transfer activity for other phospholipids and cholesterol. *J. Biol. Chem.* **252:** 1613–1619.

Bult, C.J., O. White, G.J. Olsen, L. Zhou, R.D. Fleischmann, G.G. Sutton, J.A. Blake, L.M. Fitzgerald, R.A. Clayton, J.D. Gocayne, A.R. Kerlavage, B.A. Dougherty, J.F. Tomb, M.D. Adams, C.I. Reich, R. Overbeek, E.F. Kirkness, K.G. Weinstock, J.M. Merrick, A. Glodek, J.L. Scott, N.S.M. Geoghagen, J.F. Weidman, J.L. Fuhrmann, J.C. Venter, et al. 1996. Complete genome sequence of the methanogenic archaeon, *Methanococcus jannaschii. Science* **273:** 1058–1073.

Bunya, M., M. Maebuchi, T. Hashimoto, S. Yokota, and T. Kamiryo. 1997. A second isoform of 3-ketoacyl-CoA thiolase found in *Caenorhabditis elegans,* which is similar to sterol carrier protein-x but lacks the sequence of sterol carrier protein-2. *Eur. J. Biochem.* **245:** 252–259.

Chanderbhan, R., B.J. Noland, T.J. Scallen, and G.V. Vahouny. 1982. Sterol carrier protein-2—Delivery of cholesterol from adrenal lipid droplets to mitochondria for pregnenolone synthesis. *J. Biol. Chem.* **257:** 8928–8934.

Chomczynski, P. and N. Sacchi. 1987. Single-step method of RNA isolation by acid guanidinium thiocyanate phenol chloroform extraction. *Anal. Biochem.* **162:** 156–159.

Croes, K., P.P. van Veldhoven, G.P. Mannaerts, and M. Casteels. 1997. Production of formyl-CoA during peroxisomal alpha-oxidation of 3-methyl-branched fatty acids. *FEBS Lett.* **407:** 197–200.

Fort, P., L. Marty, M. Piechaczyk, S. el Sabrouty, C. Dani, P. Jeanteur, and J.M. Blanchard. 1985. Various rat adult tissues express only one major mRNA species from the glyceraldehyde-3-phosphate-dehydrogenase multigenic family. *Nucleic Acids Res.* **13:** 1431–1442.

Hijikata, M., N. Ishii, H. Kagamiyama, T. Osumi, and T. Hashimoto. 1987. Structural analysis of cDNA for rat peroxisomal 3-ketoacyl-CoA thiolase. *J. Biol. Chem.* **262:** 8151–8158.

Hirai, A., T. Kino, K. Tokinaga, K. Tahara, Y. Tamura, and S. Yoshida. 1994. Regulation of sterol carrier protein-2 (SCP2) gene-expression in rat peritoneal-macrophages during foam cell-formation—A key role for free-cholesterol content. *J. Clin. Invest.* **94:** 2215–2223.

Hooper, M., K. Hardy, A. Handyside, S. Hunter, and M. Monk. 1987. HPRT-deficient (Lesch-Nyhan) mouse embryos derived from germline colonization by cultured cells. *Nature* **326:** 292–295.

Keller, G.A., T.J. Scallen, D. Clarke, P.A. Maher, S.K. Krisans, and S.J. Singer. 1989. Subcellular-localization of sterol carrier protein-2 in rat hepatocytes—Its primary localization to peroxisomes. *J. Cell Biol.* **108:** 1353–1361.

Laird, P.W., A. Zijderveld, K. Linders, M.A. Rudnicki, R. Jaenisch, and A. Berns. 1991. Simplified mammalian DNA isolation procedure. *Nucleic Acids Res.* **19:** 4293.

Leenders, F., J.G. Tesdorpf, M. Markus, T. Engel, U. Seedorf, and J. Adamski. 1996. Porcine 80-kda protein reveals intrinsic 17-beta-hydroxysteroid dehydrogenase, fatty acyl-CoA-hydratase/dehydrogenase, and sterol transfer activities. *J. Biol. Chem.* **271:** 5438–5442.

Lemberger, T., B. Desvergne, and W. Wahli. 1996. Peroxisome proliferator-activated receptors: a nuclear receptor signaling pathway in lipid physiology. *Ann. Rev. Cell Dev. Biol.* **12:** 335–363.

McLean, M.P., J.T. Billheimer, K.J. Warden, and R.B. Irby. 1995. Differential expression of hepatic sterol carrier proteins in the streptozotocin-treated diabetic rat. *Endocrinology* **136:** 3360–3368.

Noland, B.J., R.E. Arebalo, E. Hansbury, and T.J. Scallen. 1980. Purification and properties of sterol carrier protein-2. *J. Biol. Chem.* **255:** 4282–4289.

Ohba, T., H. Rennert, S.M. Pfeifer, Z.G. He, R. Yamamoto, J.A. Holt, J.T. Billheimer, and J.F. Strauss. 1994. The structure of the human sterol carrier protein-x/sterol carrier protein-2 gene (scp2). *Genomics* **24:** 370–374.

Ohba, T., J.A. Holt, J.T. Billheimer, and J.F. Strauss. 1995. Human sterol carrier protein-x/sterol carrier protein-2 gene has two promoters. *Biochemistry* **34:** 10660–10668.

Ossendorp, B.C. and K.W.A. Wirtz. 1993. The nonspecific lipid-transfer protein (sterol carrier protein-2) and its relationship to peroxisomes. *Biochimie* **75:** 191–200.

Ossendorp, B.C., G.P.H. van Heusden, A.L.J. de Beer, K. Bos, G.L. Schouten, and K.W.A. Wirtz. 1991. Identification of the cDNA clone which encodes the 58-kda protein containing the amino-acid-sequence of rat-liver nonspecific lipid- transfer protein (sterol carrier protein-2)—Homology with rat peroxisomal and mitochondrial 3-oxoacyl-CoA thiolases. *Eur. J. Biochem.* **201:** 233–239.

Pfeifer, S.M., E.E. Furth, T. Ohba, Y.J. Chang, H. Rennert, N. Sakuragi, J.T. Billheimer, and J.F. Strauss. 1993a. Sterol carrier protein-2—A role in steroid-hormone synthesis. *J. Steroid Biochem. Mol. Biol.* **47:** 167–172.

Pfeifer, S.M., N. Sakuragi, A. Ryan, A.L. Johnson, R.G. Deeley, J.T. Billheimer, M.E. Baker, and J.F. Strauss. 1993b. Chicken sterol carrier protein-2/sterol carrier protein-x: cDNA cloning reveals evolutionary conservation of structure and regulated expression. *Arch. Biochem. Biophys.* **304:** 287–293.

Puglielli, L., A. Rigotti, A.V. Greco, M.J. Santos, and F. Nervi. 1995. Sterol carrier protein-2 is involved in cholesterol transfer from the endoplasmic reticulum to the plasma membrane in human fibroblasts. *J. Biol. Chem.* **270:** 18723–18726.

Raabe, M., U. Seedorf, H. Hameister, P. Ellinghaus, and G. Assmann. 1996. Structure and chromosomal assignment of the murine sterol carrier protein-2 gene (Scp2) and two related pseudogenes by *in situ* hybridization. *Cytogenet. Cell Genet.* **73:** 279–281.

Rennert, H., A. Amsterdam, J.T. Billheimer, and J.F. Strauss. 1991. Regulated expression of sterol carrier protein-2 in the ovary—A key role for cyclic-AMP. *Biochemistry* **30:** 11280–11285.

Schram, A.W., S. Goldfischer, C.W. van Roermund, K.E. Brouwer, J. Collins, T. Hashimoto, H.S. Heymans, H. van den Bosch, R.B. Schutgens, J.M. Tager, et al. 1987. Human peroxisomal 3-oxoacyl-coenzyme A thiolase deficiency. *Proc. Natl. Acad. Sci.* **84:** 2494–2496.

Seedorf, U. and G. Assmann. 1991. Cloning, expression, and nucleotide-sequence of rat-liver sterol carrier protein-2 cDNAs. *J. Biol. Chem.* **266:** 630–636.

Seedorf, U., M. Raabe, and G. Assmann. 1993. Cloning, expression and sequences of mouse sterol-carrier protein-x-encoding cDNAs and a related pseudogene. *Gene* **123:** 165–172.

Seedorf, U., P. Brysch, T. Engel, K. Schrage, and G. Assmann. 1994a. Sterol carrier protein-x is peroxisomal 3-oxoacyl coenzyme-A thiolase with intrinsic sterol carrier and lipid transfer activity. *J. Biol. Chem.* **269:** 21277–21283.

Seedorf, U., S. Scheek, T. Engel, C. Steif, H.J. Hinz, and G. Assmann. 1994b. Structure-activity studies of human sterol

carrier protein-2. *J. Biol. Chem.* **269:** 2613–2618.

Seedorf, U., M. Fobker, R. Voss, K. Meyer, F. Kannenberg, D. Meschede, K. Ullrich, J. Horst, A. Benninghoven, and G. Assmann. 1995. Smith-Lemli-Opitz syndrome diagnosed by using time-of-flight secondary-ion mass-spectrometry. *Clin. Chem.* **41:** 548–552.

Singh, H. and A. Poulos. 1995. Substrate-specificity of rat-liver mitochondrial carnitine palmitoyl transferase-I—Evidence against alpha-oxidation of phytanic acid in rat-liver mitochondria. *FEBS Lett.* **359:** 179–183.

Singh, H., K. Beckman, and A. Poulos. 1994. Peroxisomal beta-oxidation of branched chain fatty acids in rat liver. Evidence that carnitine palmitoyltransferase I prevents transport of branched chain fatty acids into mitochondria. *J. Biol. Chem.* **269:** 9514–9520.

Steinberg, D. 1995. Refsum disease. In *The metabolic and molecular basis of inherited disease* (ed. C.R. Scriver, A.L. Beaudet, W.S. Sly, and D. Valle), pp. 2351–2370. McGraw-Hill, New York, NY.

Stolowich, N.J., A. Frolov, B. Atshaves, E.J. Murphy, C.A. Jolly, J.T. Billheimer, A.I. Scott, and F. Schroeder. 1997. The sterol carrier protein-2 fatty acid binding site: an NMR, circular dichroic, and fluorescence spectroscopic determination. *Biochemistry* **36:** 1719–1729.

Trzeciak, W.H., E.R. Simpson, T.J. Scallen, G.V. Vahouny, and M.R. Waterman. 1987. Studies on the synthesis of sterol carrier protein-2 in rat adrenocortical-cells in monolayer-culture-regulation by ACTH and dibutyryl cyclic 3′,5′-AMP. *J. Biol. Chem.* **262:** 3713–3717.

Wanders, R.A., C.W.T. van Roermund, D.S.M. Schor, H.J. Tenbrink, and C. Jakobs. 1994. 2-hydroxyphytanic acid oxidase activity in rat and human liver and its deficiency in the Zellweger-syndrome. *Biochim. Biophys. Acta Mol. Basis Dis.* **1227:** 177–182.

Wanders, R.A., S. Denis, F. Wouters, K.W.A. Wirtz, and U. Seedorf. 1997. Sterol carrier protein-x (SCPx) is a peroxisomal branched-chain beta-ketothiolase specifically reacting with 3-oxo-pristanoyl-CoA: A new, unique role for SCPx in branched-chain fatty acid metabolism in peroxisomes. *Biochem. Biophys. Res. Commun.* **236:** 565–569.

Watkins, P.A., A.E. Howard, and S.J. Mihalik. 1994. Phytanic acid must be activated to phytanoyl-CoA prior to its alpha-oxidation in rat liver peroxisomes. *Biochim. Biophys. Acta* **1214:** 288–294.

Watkins, P.A., A.E. Howard, S.J. Gould, J. Avigan, and S.J. Mihalik. 1996. Phytanic acid activation in rat liver peroxisomes is catalyzed by long-chain acyl-CoA synthetase. *J. Lipid Res.* **37:** 2288–2295.

Xu, T.S., E.P. Bowman, D.B. Glass, and J.D. Lambeth. 1991. Stimulation of adrenal mitochondrial cholesterol side-chain cleavage by GTP, steroidogenesis activator polypeptide (SAP), and sterol carrier protein-2. *J. Biol. Chem.* **266:** 6801–6807.

Yamamoto, R., C.B. Kallen, G.O. Babalola, H. Rennert, J.T. Billheimer, and J.F. Strauss. 1991. Cloning and expression of a cDNA encoding human sterol carrier protein-2. *Proc. Natl. Acad. Sci.* **88:** 463–467.

Yanase, T., T. Hara, Y. Sakai, R. Takayanagi, and H. Nawata. 1996. Expression of sterol carrier protein-2 (SCP2) in human adrenocortical tissue. *Eur. J. Endocrinol.* **134:** 501–507.

Zhang, S.H., R.L. Reddick, J.A. Piedrahita, and N. Maeda. 1992. Spontaneous hypercholesterolemia and arterial lesions in mice lacking apolipoprotein-E. *Science* **258:** 468–471.

Defective peroxisomal catabolism of branched fatty acyl coenzyme A in mice lacking the sterol carrier protein-2/sterol carrier protein-x gene function

Udo Seedorf, Martin Raabe, Peter Ellinghaus, et al.

Genes Dev. 1998, **12:**